

# Effect of Calcium Promoters on Nanostructured Iron Catalyst for Fischer-Tropsch Synthesis

Yahya Zamani\*, Akbar Zamaniyan, Farzad Bahadoran, and Mehrdad Shojaei

Research Institute of Petroleum Industry (RIPI), National Iranian Oil Company, West Blvd. of Azadi Sports Complex, P.O.BOX 14665-137, Tehran, Iran

## ABSTRACT

The Fischer-Tropsch synthesis (FTS) has been recognized as a heterogeneous surface-catalyzed polymerization process. During this process,  $\text{CH}_x$  monomers formed via the hydrogenation of adsorbed CO on transition metals produce hydrocarbons and oxygenates with a broad range of chain lengths and functional groups. A series of Fe/Cu Fischer-Tropsch synthesis catalysts incorporated with a calcium promoter were prepared by a microemulsion method. The composition of the final nanosized iron catalysts in terms of the atomic ratio is as follows: 100Fe/4Cu, 100Fe/4Cu/2Ca, 100Fe/4Cu/4Ca. XRD, BET, TEM, and TPR techniques were used to study the catalysts phase, structure, and morphology. Fischer-Tropsch synthesis (FTS) reaction test was performed in a fixed bed reactor. All the promoted catalysts, compared to the unpromoted catalysts, have higher rates of FT and the secondary reaction for  $\text{CO}_2$  production. The formation of methane and light hydrocarbons is restrained with increasing the amount of calcium. The 100Fe/4Cu/2Ca shows the best performance between the prepared catalysts.

**Keywords:** Nanoparticle Iron Catalyst, Fischer-Tropsch Synthesis, Calcium Promoter

## INTRODUCTION

High energy cost is the main driving force behind currently increasing interest in the Fischer-Tropsch synthesis (FTS) for the conversion of natural gas to liquids (GTL). The catalytic synthesis of hydrocarbons from CO and  $\text{H}_2$  syngas mixtures leads to a large variety of products such as paraffins, olefins, alcohols, and aldehydes. Several metal catalysts can be used for the FTS; however, only iron and cobalt catalysts appear to be economically feasible on an industrial scale [1]. Cobalt catalysts yield mainly straight-chain hydrocarbons [2,3], while iron catalysts are more useful either when the  $\text{H}_2/\text{CO}$  ratio is

low because of the water-gas shift (WGS) activity of Fe or for the production of alkenes, oxygenates, and branched hydrocarbons, which depends on the promoters and process conditions employed [2,4]. Most of the studies reported have attempted to improve catalyst performance by promoting with additives such as K [5,6], Mn [7], Cr [5], Ru [8], and Pt [9]. Among promoters, potassium has been used as a promoter for iron catalysts. Potassium can also increase the catalytic activity in FTS and WGS reactions [10,11]. Copper is normally added to Fe-based Fischer-Tropsch synthesis (FTS) catalysts as a chemical promoter; it is added to enhance hematite reducibility [10]. Very stable

### \*Corresponding author

Yahya Zamani  
Email: yahyazamani@yahoo.com  
Tel: +98 21 4825 3354  
Fax: +98 21 4473 9716

### Article history

Received: June 25, 2013  
Received in revised form: September 28, 2013  
Accepted: October 22, 2013  
Available online: February 20, 2015

activity and high selectivity to light olefin formation have been observed for Mn-promoted Fe catalysts [12,13]. A positive effect of other transition metals such as La, Mo, Ta, V, and Zr on the catalyst activity for both CO hydrogenation and WGS activity has also been reported [14-17]. Although the studies on the Fe-based FT catalysts are extensive, the investigations on the effect of calcium on the catalyst are scarce and the effect of calcium on the nanosized iron-based catalysts has not been investigated. In this study, a microemulsion method has been developed to prepare three nanosized iron catalysts by preparing nanosized iron with copper and calcium oxide separately from their solutions. The objective of this work is to investigate the effect of calcium promoter on catalyst morphology, activity, and product selectivity in Fischer-Tropsch synthesis. The catalysts were tested in a fixed bed stainless steel reactor at FTS conditions.

## EXPERIMENTALS

### Catalyst Preparation

Nanostructured iron catalysts were prepared by a microemulsion method. A water solution of metal precursors,  $\text{FeCl}_3 \cdot 6\text{H}_2\text{O}$  and  $\text{Cu}(\text{NO}_3)_2 \cdot 4\text{H}_2\text{O}$  were added to a mixture of 2-propanol and chloroform with a ratio of 1:1 and sodium dodecyl sulfate (SDS) as a surfactant. Hydrazine (25-30%) in the aqueous phase was added as a precipitating agent and stirred for 4 hours. The solid was recovered by centrifugation and washed thoroughly with distilled water, ethanol, and acetone. Finally, the samples were dried overnight at 110 °C, and subsequently calcined in air at 380 °C for 4 hrs. Nanostructured calcium oxide was prepared like nanostructured Fe-Cu. At the next step, they were mixed together. The promoted catalysts were dried at 110 °C for 15 hrs and calcined at 380 °C for 4 hrs in air [16,17]. The catalyst compositions were designated in terms of the atomic ratios as: 100Fe/4Cu, 100Fe/4Cu/ 2Ca, and 100Fe/4Cu/4Ca. All the

samples were pressed into pellets, crushed, and sieved to obtain particles with 30-40 mesh.

### Catalyst Characterization

BET surface area and the pore volume of the catalysts were determined by  $\text{N}_2$  physisorption using a Micromeritics ASAP 2010 automated system. A 0.3 g catalyst sample was degassed in the system at 100 °C for 1 hr and then at 300 °C for 2 hrs prior to analysis. The analysis was done using  $\text{N}_2$  adsorption at 196 °C. The average particle size of the calcined powders was measured by LEO 912AB TEM. The XRD spectra of the fresh catalyst were conducted with a Philips PW1840 X-ray diffractometer with monochromatized Cu ( $K\alpha$ ) radiation for determining iron phases. Temperature programmed reduction (TPR) profiles of the calcined catalysts were recorded using a Micromeritics TPD-TPR 290 system. The TPR of 50 mg of each sample was performed in 5% hydrogen/argon gas mixture. The samples were heated from 50 to 900 °C at a heating rate of 10 °C/min. The  $\text{H}_2$  reduction process illustrated three stages in the temperature range between 200-900 °C.

### Reactor System and Operation Procedure

The catalytic reaction experiments were conducted in a fixed bed stainless steel reactor. The flow rate of inlet gases and reactor pressure were controlled by electronic mass flow and pressure controllers respectively. A four heating zone furnace with a temperature controller and indicator supplied the required reaction heat. The reactor was loaded by 1 g of catalyst. The catalyst was reduced in a 10%  $\text{H}_2/\text{N}_2$  flow for 3 hrs. The catalyst activation was followed in a stream of synthesis gas with  $\text{H}_2/\text{CO} = 1$  and  $\text{SV} = 1.5 \text{ nl.h}^{-1}.\text{gcat}^{-1}$  for 24 hrs at atmospheric pressure and a temperature of 270 °C. Following the activation process, the reactor pressure and temperature raised to 17 bar and 290°C respectively and the reaction was initiated in

synthesis gas stream with  $H_2/CO = 1$  and  $GHSV = 3$   $nl.h^{-1}.gCat^{-1}$ . The products were analyzed by two gas chromatographs (Varian CP 3800), one of which was equipped with two subsequent connected columns. The two packed columns connected to two thermal conductivity detectors (TCD) were used for analyzing  $H_2$ ,  $CO$ ,  $CO_2$ ,  $CH_4$ , and other non-condensable gases and the other one with a Petrocol Tm DH100 fused silica capillary column attached to a flame ionization detector (FID) was used for analyzing organic liquid products [18,19]. The activities and product selectivity were assessed after 72 hrs from the initial time.

## RESULTS AND DISCUSSION

Alkaline elements are used as promoters because they can modify the adsorption pattern of the reactants ( $H_2$  and  $CO$ ) on the active sites. The overall effects of these promoters, such as potassium, on the behavior of the iron-based FTS catalysts, namely  $CO$  chemisorptions enhancement, have been justified as a consequence of the iron tendency to withdraw electronic density from potassium. Therefore, the strength of the  $Fe-CO$  bond was enhanced [18]. While alkali loading is high,  $CO$  dissociation proceeds faster than carbon hydrogenation, which causes an excessive carbon deposition and consequently deactivates the catalyst surface ultimately [20]. Table 1 shows the results of catalysts surface area. By adding calcium, the BET surface area and pore volume of the catalysts decrease as it promotes the aggregation of the catalyst crystallites and blocks up the pore volume of the catalyst.

Nanostructured iron catalysts were characterized by X-ray diffraction (XRD) after calcinations. Figure 1 shows the XRD patterns of the catalysts prepared by the microemulsion method. The addition of  $Ca$  did not cause any obvious changes and no phase containing metals were detected. All the catalysts showed the  $Fe_2O_3$  crystalline phase; however, their structure

seemed to be like cubic hematite structured  $Fe_2O_3$  crystal in JCPDS database.

Table 1: Catalysts surface area

Catalysts	BET Surface area( $m^2/g$ )	Pore Volume ( $cm^3/g$ )
100Fe/4Cu	49.3	0.26
100Fe/4Cu/2Ca	45.5	0.23
100Fe/4Cu/4Ca	41.2	0.19

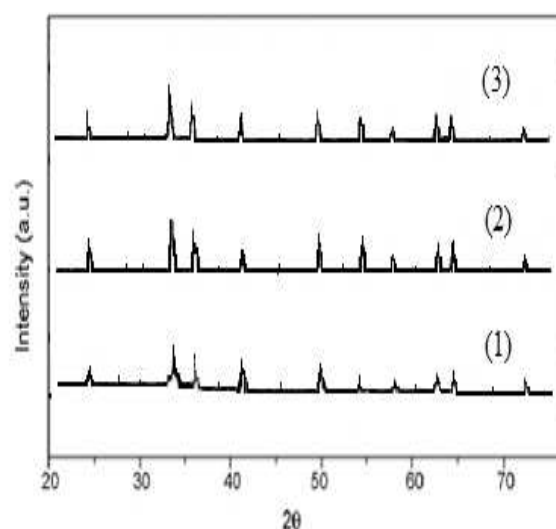


Figure 1: XRD spectra of the fresh catalysts: (1) 100Fe/4Cu; (2) 100Fe/4Cu/2Ca; (3) 100Fe/4Cu/4Ca.

The morphology of the catalysts was illustrated by TEM images as shown in Figure 2. Although TEM revealed that the nanoparticle diameter was in the range of 10-40 nm, difference between the catalysts with diverse ratios of metal oxides was obscured.

Figure 3 shows the  $H_2$ -TPR profiles of the nanosized iron catalysts.  $H_2$ -TPR determines the reduction behavior of the catalysts. The first stage is ascribed to the transformations of  $CuO$  to  $Cu$ , and the second stage is attributed to the transformation of  $Fe_2O_3$  to  $Fe_3O_4$ , whereas the third stage represents the transformation of  $Fe_3O_4$  to  $Fe$ .

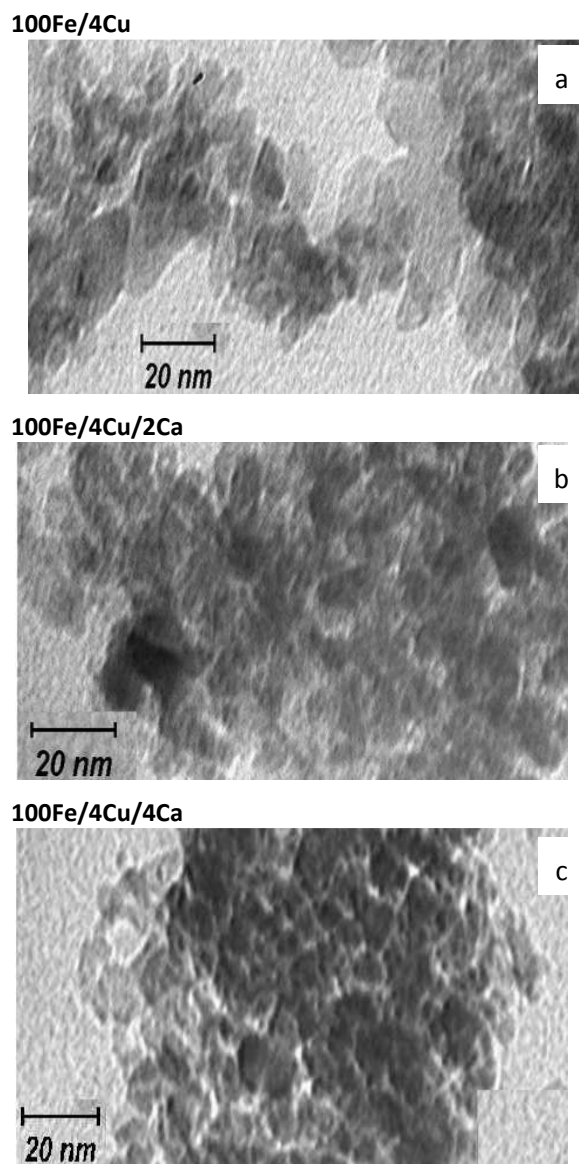


Figure 2: TEM micrographs of the catalysts

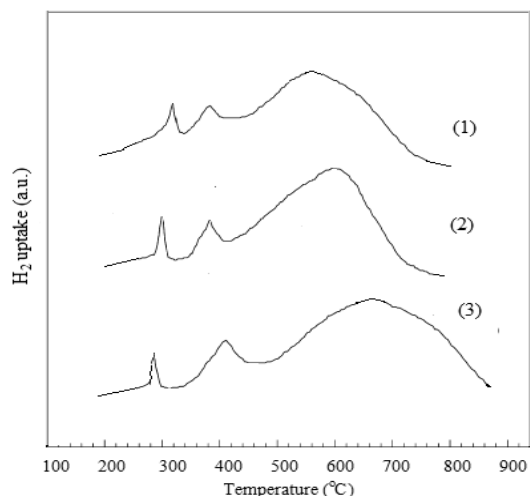


Figure 3: H<sub>2</sub>-TPR profiles of the catalysts: (1) 100Fe/4Cu; (2) 100Fe/4Cu/2Ca; (3) 100Fe/4Cu/4Ca.

An increase in the concentration of the promoter led to an increase in the reduction temperature and reaction time. Figure 4 shows the rates of FTS and WGS.

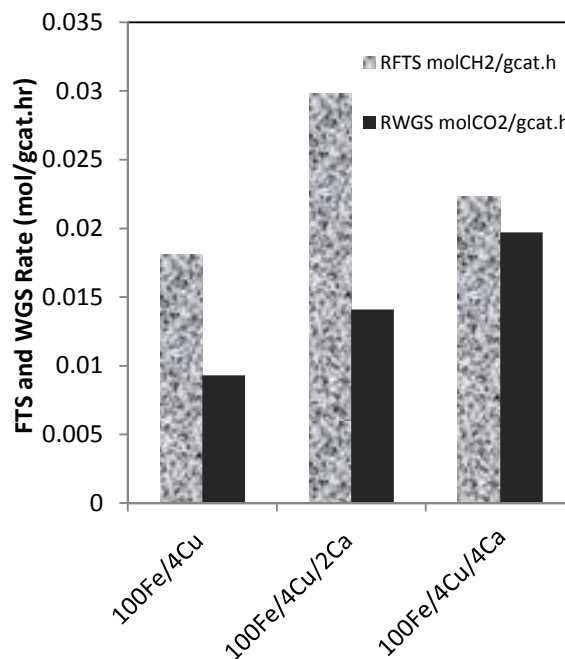


Figure 4:  $R_{FTS}$  and  $R_{WGS}$  of the catalysts

The addition of promoter increases the catalyst activity, whereas the addition of copper accelerates the deactivation of the catalyst; the addition of calcium as a promoter apparently improves the FTS activity of iron-based catalysts. However, the promoted iron catalysts have higher rates of FTS and WGS than the unpromoted catalyst.

H<sub>2</sub>O plays an important role in changing the iron phase composition during the FTS process. A reversible WGS reaction accompanying the FTS reaction over iron-based catalyst is recognized well (Equations 1 and 2) [21]:

$$r_{WGS} = r_{CO_2} \quad (1)$$

and

$$r_{FTS} = r_{CO} - r_{WGS} \quad (2)$$

As the WGS reaction needs the water produced by the FTS, an inequality is always observed:

$$r_{\text{WGS}} \leq r_{\text{FTS}} \quad (3)$$

During the FTS process, one part of  $\text{H}_2\text{O}$  produced by FTS reaction is consumed by WGS reaction, whereas the remainder is left in the reactor and keeps certain pressure of water vapor.

$\text{Fe}_3\text{O}_4$  is the active site for WGS reaction on iron-based catalyst [22], while calcium is an only electronic promoter. The incorporation of calcium promoter into iron-based catalyst can promote CO adsorption, increases the concentration of CO species, shifts WGS reaction forwards and thus improves WGS activity. The high WGS activity decreases the  $\text{H}_2\text{O}$  pressure and stabilizes the iron carbides [23]. CO conversion and the products selectivity of the catalysts are displayed in Figure 5.

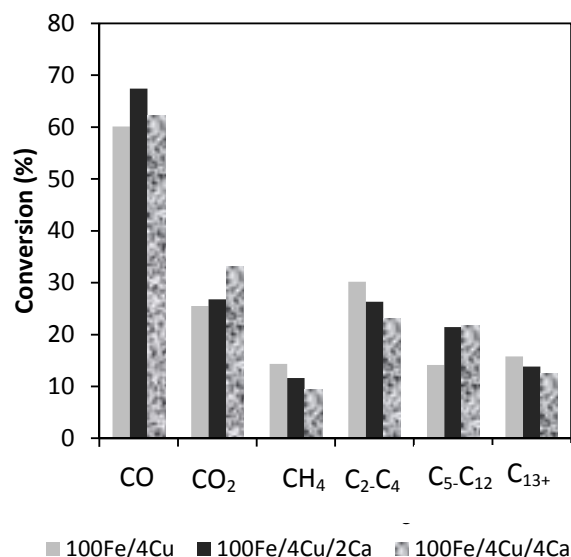


**Figure 5: Product selectivity of the catalysts; Reaction condition: Time on Stream 72 hrs, 290 °C, 1.7 MPa,  $\text{H}_2/\text{CO} = 1$ , and  $\text{SV} = 3 \text{nl.gCat}^{-1}.\text{hr}^{-1}$ .**

Figure 5 shows the selectivity in gaseous and light hydrocarbons (methane and  $\text{C}_2\text{-C}_4$ ) and heavy hydrocarbons ( $\text{C}_{5+}$ ). It should be noted that the selectivity of oxygenates was negligible (<3%) in all the cases. The addition of the Ca promoter with a content of 2% led to an increase in CO conversion, but higher concentration up to 4% decreased the CO conversion. The higher hydrocarbon selectivity increased with increasing calcium oxide content. However, the selectivities

of methane and light weight hydrocarbons ( $\text{C}_2\text{-C}_4$ ) showed an opposite trend with respect to  $\text{C}_{5+}$  selectivity. All of these results imply that the hydrogenation reaction was decreased while the promoter was added to the catalyst. Both the amount of the promoter and the reaction conditions influenced the product selectivity. The results showed that the addition of the promoter facilitated the CO dissociative adsorption, leading to a higher deposition of carbon species on the surface.

## CONCLUSIONS

Nanostructured iron catalysts were prepared by a microemulsion method. A series of unpromoted and CaO-promoted iron nanocatalysts were studied using different characterization techniques. The effect of calcium oxide on the Fischer-Tropsch synthesis activity and selectivity was investigated in a fixed bed reactor. It was shown that the activity and  $\text{C}_{5+}$  selectivity increased, but methane selectivity decreased with increasing the amount of calcium oxide, which was attributed to the increased reducibility. The changes in the catalytic performances could be ascribed to the effect of the promoter on  $\text{H}_2$  and CO adsorption, which further affected the FTS performances of the catalysts significantly.

## ACKNOWLEDGMENT

We are grateful to the Research and Development of National Iranian Oil Company (NIOC) for the financial support of the current work.

## REFERENCES

- [1] Rao V. U. S., Stiegel G. J., Cinquegrane G. J., and Srivastava R. D., "Iron-based Catalysts for Slurry-phase Fischer-Tropsch Process: Technology Review," *Fuel Process. Technol.*, **1992**, *30*, 83-107.
- [2] O'Brien R. J., Xu L., Spicer R. L., Bao S., et al., "Activity and Selectivity of Precipitated Iron Fischer-Tropsch Catalysts," *Catal. Today*, **1997**, *36*, 325-334.
- [3] Panpranot J., Kaewkun S., Praserttham P.,

<http://jpest.ripi.ir>

- and Goodwin J. G., "Effect of Cobalt Precursors on the Dispersion of Cobalt on MCM-41," *Catal. Lett.*, **2003**, *91*, 95-102.
- [4] Mills G. A., "Catalysts for Fuels from Syngas," *IEA Coal Research*, London, **1988**, 34-44.
- [5] Duvenhage D. J. and Coville N. J., "Effect of K, Mn and Cr on the Fischer-Tropsch Activity of Fe:Co/TiO<sub>2</sub> Catalysts," *Catal. Lett.*, **2005**, *104*, 129-133.
- [6] Yang Y., Xiang H. W., Xu Y. Y., Bai L., et al., "Effect of Potassium Promoter on Precipitated Iron-manganese Catalyst for Fischer-Tropsch Synthesis," *Appl. Catal. A*, **2004**, *266*, 181-194.
- [7] Li T., Yang Y., Zhang C., An X., et al., "Effect of Manganese on an Iron-based Fischer-Tropsch Synthesis Catalyst Prepared from Ferrous Sulfate," *Fuel.*, **2007**, *86*, 921-928.
- [8] Li S., Krishnamoorthy S., Li A., Meitzner G. D., et al., "Promoted Iron-based Catalysts for the Fischer-Tropsch Synthesis: Design, Synthesis, Site Densities, and Catalytic Properties," *J. Catal.*, **2002**, *206*, 202-217.
- [9] Yu W., Wu B., Xu J., Tao Z., et al., "Effect of Pt Impregnation on a Precipitated Iron-based Fischer-Tropsch Synthesis Catalyst," *Catal. Lett.*, **2008**, *125*, 116-122.
- [10] Li S., Li A., Krishnamoorthy S., and Iglesia E., "Effects of Zn, Cu, and K Promoters on the Structure and on the Reduction, Carburization, and Catalytic Behavior of Iron-based Fischer-Tropsch Synthesis Catalysts," *Catal. Lett.*, **2001**, *77*, 197-205.
- [11] Fazlollahi F., Sarkari M., Gharebaghi H., Atashi H., et al., "Preparation of Fe-Mn/K/Al<sub>2</sub>O<sub>3</sub> Fischer-Tropsch Catalyst and Its Catalytic Kinetics for the Hydrogenation of Carbon Monoxide," *Chin. J. Chem. Eng.*, **2013**, *21*, 507-519.
- [12] Bai L., Xiang H. W., Li Y. W., Han Y. Z., et al., "Slurry Phase Fischer-Tropsch Synthesis over Manganese-promoted Iron Ultrafine Particle Catalyst," *Fuel.*, **2002**, *81*, 1577-1581.
- [13] Tao Z., Yang Y., Wan H., Li T., et al., "Effect of Manganese on a Potassium-promoted Iron-based Fischer-Tropsch Synthesis Catalyst," *Catalysis Letters.*, **2007**, *114*, 161-168.
- [14] Nattaporn L., James G., and Edgar L., "Fe-based Fischer-Tropsch Synthesis Catalysts Containing Carbide-forming Transition Metal Promoters," *Journal of Catalysis*, **2008**, *255*, 104-113.
- [15] Feyzi M., Irandoust M., and Mirzaei A. A., "Effects of Promoters and Calcinations Conditions on the Catalytic Performance of Iron-manganese Catalysts for Fischer-Tropsch Synthesis," *Fuel. Pro. Tech.*, **2011**, *92*, 1136-1143.
- [16] Nakhaei Pour A., Taghipoor S., Shekarriz M., Shahri S. M. K., et al., "Fischer-Tropsch Synthesis with Fe/Cu/La/SiO<sub>2</sub> Nanostructured Catalyst," *J. Nanosci. Nanotech.*, **2008**, *8*, 1-5.
- [17] Zamani Y., Bakavoli M., Rahimizadeh M., Mohajeri A., et al., "Synergetic Effect of La and Ba Promoters on Nanostructured Iron Catalyst in Fischer-Tropsch Synthesis," *Chin. J. Catal.*, **2012**, *33*, 1119-1124.
- [18] Zamani Y., Yousefian S. H., Pour A. N., Moshtari B., et al., "A Method for the Regeneration of Used Fe-ZSM<sub>5</sub> Catalyst in Fischer-Tropsch Synthesis," *Chem. Eng. Trans.*, **2010**, *21*, 1045-1051.
- [19] Nakhaei Pour A., Kamali Shahri S. M., Bozorgzadeh H. R., Zamani Y., et al., "Effect of Mg, La and Ca Promoters on the Structure and Catalytic Behavior of Iron-based Catalysts in Fischer-Tropsch Synthesis," *Appl. Catal. A: Gen.*, **2008**, *348*, 201-208.
- [20] Herranz T., Rojas S., Pe' rez-Alonso F. J., Ojeda M., et al., "Hydrogenation of Carbon Oxides over Promoted Fe-Mn Catalysts Prepared by the Microemulsion Methodology," *Appl. Catal. A*, **2006**, *311*, 66-75.
- [21] Bukur D. B., Nowicki L., Manne R. K., and Lang X. S., "Activation Studies with a Precipitated Iron Catalyst for Fischer-Tropsch Synthesis: II Reaction Studies," *J. Catal.*, **1995**, *155*, 366-375.
- [22] Li S., O'Brien R. J., Meitzner G. D., Hamdeh

H., et al., "Structural Analysis of Unpromoted Fe-based Fischer-Tropsch Catalysts Using X-ray Absorption Spectroscopy," *Appl. Catal. A: Gen.*, **2001**, 219, 215-222.

[23] Yang Y., Xiang H. W., Xu Y. Y., Bai L., et al., "Effect of Potassium Promoter on Precipitated Iron-manganese Catalyst for Fischer-Tropsch Synthesis," *Appl. Catal. A: Gen.*, **2004**, 266, 181-194.